J Neurophysiol 103: 1646–1657, 2010.
First published January 20, 2010; doi:10.1152/jn.00950.2009.

Processing of Horizontal Optic Flow in Three Visual Interneurons of the *Drosophila* Brain

B. Schnell,[1] M. Joesch,[1] F. Forstner,[1] S. V. Raghu,[1] H. Otsuna,[2] K. Ito,[2] A. Borst,[1] and D. F. Reiff[1]

[1]*Department of Systems and Computational Neurobiology, Max Planck Institute of Neurobiology, Martinsried, Germany; and* [2]*Center for Bioinformatics, Institute of Molecular and Cellular Biosciences, University of Tokyo, Tokyo, Japan*

Submitted 27 October 2009; accepted in final form 17 January 2010

Schnell B, Joesch M, Forstner F, Raghu SV, Otsuna H, Ito K, Borst A, Reiff DF. Processing of horizontal optic flow in three visual interneurons of the *Drosophila* brain. *J Neurophysiol* 103: 1646–1657, 2010. First published January 20, 2010; doi:10.1152/jn.00950.2009. Motion vision is essential for navigating through the environment. Due to its genetic amenability, the fruit fly *Drosophila* has been serving for a lengthy period as a model organism for studying optomotor behavior as elicited by large-field horizontal motion. However, the neurons underlying the control of this behavior have not been studied in *Drosophila* so far. Here we report the first whole cell recordings from three cells of the horizontal system (HSN, HSE, and HSS) in the lobula plate of *Drosophila.* All three HS cells are tuned to large-field horizontal motion in a direction-selective way; they become excited by front-to-back motion and inhibited by back-to-front motion in the ipsilateral field of view. The response properties of HS cells such as contrast and velocity dependence are in accordance with the correlation-type model of motion detection. Neurobiotin injection suggests extensive coupling among ipsilateral HS cells and additional coupling to tangential cells that have their dendrites in the contralateral hemisphere of the brain. This connectivity scheme accounts for the complex layout of their receptive fields and explains their sensitivity both to ipsilateral and to contralateral motion. Thus the main response properties of *Drosophila* HS cells are strikingly similar to the responses of their counterparts in the blowfly *Calliphora*, although we found substantial differences with respect to their dendritic structure and connectivity. This long-awaited functional characterization of HS cells in *Drosophila* provides the basis for the future dissection of optomotor behavior and the underlying neural circuitry by combining genetics, physiology, and behavior.

INTRODUCTION

Flies rely heavily on visual motion information to navigate safely through the environment (Borst and Haag 2002). Once airborne, they use the characteristic flow fields caused by their self-motion to correct for deviations from a straight flight path. The precision and reliability of these so-called optomotor responses, combined with the small size of their brain, make flies an ideal organism to study the underlying neural circuitry (Chan et al. 1998; Egelhaaf et al. 2003; Frye and Dickinson 2001; Götz 1964; Heisenberg et al. 1978).

Detailed anatomical maps describing the cell types of the optic lobes (Fischbach and Dittrich 1989; Scott et al. 2002; Strausfeld 1976) are at hand. In the blowfly *Calliphora*, about 60 motion sensitive neurons, the so-called lobula plate tangential cells (LPTCs), extract information about large- and small-field motion from the optic flow. Some LPTCs synapse directly onto descending neurons to ultimately control head movement and locomotion (Chan et al. 1998; Gilbert et al. 1995; Gronenberg and Strausfeld 1990).

To analyze neuronal function different approaches were pursued in large and small flies. In *Calliphora* the response properties of LPTCs have been characterized in greatest detail by intracellular recording (Borst and Haag 2002). Among them, cells of the vertical system (VS) respond preferentially to vertical motion (Hengstenberg et al. 1982) and motion elicited by rotation around an axis in the horizontal plane of the animal (Krapp et al. 1998). Horizontal system (HS) cells respond to translation (Hausen 1982a,b) and rotational motion around the vertical axis of the fly (Krapp et al. 2001). Their tuning to specific optic flow fields can be explained by dendritic input from opposing arrays of local motion detectors built from columnar elements (Borst and Egelhaaf 1990; Joesch et al. 2008; Raghu et al. 2007, 2009; Single and Borst 1998) as well as input from other LPTCs (Elyada et al. 2009; Farrow et al. 2005, 2006; Haag and Borst 2004, 2007, 2008).

In *Drosophila*, mainly genetic techniques have been used to disrupt parts of the circuitry and to compare the behavior of wild-type and mutant flies (Götz 1964, 1965; Heisenberg 1972; Heisenberg and Buchner 1977). This approach also allows one to study the functional role of small columnar neurons in the medulla presynaptic to LPTCs that could not be recorded electrically so far. In large flies some example recordings (Douglass and Strausfeld 1995, 1996, 2003; Gilbert and Strausfeld 1991) of a small number of the about 50 different columnar neurons could be obtained. Yet, their small size and the low feasibility of this approach did not provide an exhaustive picture of the cellular mechanisms of visual motion detection in the medulla of dipteran flies.

Recent studies on the behavior of wild-type (Duistermars et al. 2007; Fry et al. 2009; Mronz and Lehmann 2008; Tammero et al. 2004) and transgenic *Drosophila* with certain types of columnar neurons blocked (Katsov and Clandinin 2008; Rister et al. 2007; Zhu et al. 2009) provided new insights into motion vision and optomotor behavior. However, these studies also revealed the limitations of behavioral experiments as read-out for the functional role of a specific class of neurons. Moreover, the interpretation of such studies in *Drosophila* relies heavily on physiological data from large flies because only one functional description of LPTCs in *Drosophila* is available so far (Joesch et al. 2008).

We close this gap by characterizing the response properties of the three HS cells in *Drosophila* that are supposed to mediate yaw-turning behavior. We show that their dendritic structure and connectivity to other LPTCs are different com-

Address for reprint requests and other correspondence: D. F. Reiff, Max Planck Institute of Neurobiology, Department of Systems and Computational Neurobiology, Am Klopferspitz 18, 82152 Martinsried, Germany (E-mail: reiff@neuro.mpg.de).

pared with those of large flies. Nevertheless, their complex receptive fields, contrast dependence, and velocity tuning corroborate findings on HS cells in *Calliphora*. HS cells in *Drosophila* are similarly tuned to rotational large-field horizontal motion and match the predictions of a correlation-type model of visual motion detection.

METHODS

Flies

Flies were raised on standard cornmeal-agar medium with a 12-h light/12-h dark cycle, 25°C, and 60% humidity. We used female experimental flies, 1 day after eclosion. The line NP 0282 (established by the NP consortium; for screening see Otsuna and Ito 2006) expresses Gal4 in two of the three HS cells (HSN and HSE, Fig. 1*A*) and in unidentified neurons of the central brain. UAS-mCD8-GFP was used to highlight entire cells and UAS-mCD8-TN-XL-8aa (Joesch et al. 2008) was used to predominantly label cell bodies.

Visually guided whole cell recording

Patch-clamp recordings were performed as described previously (Joesch et al. 2008). Flies were anesthetized on ice and waxed on a Plexiglas holder. The head was bent down to expose the caudal backside of the head and the extended proboscis was fixed. Aluminum foil with a hole of about 1–2 mm sustained by a ring-shaped metal holder was placed on top of the fly and separated the upper wet part (covered with Ringer solution; Wilson et al. 2004) of the preparation from the lower dry part. Water-immersion optics was used from above; visual patterns (see following text) were presented to dry and fully intact compound eyes. A small window was cut into the backside of the head, and during mild protease treatment (protease XIV, E.C.3.4.24.31, P-5147; Sigma–Aldrich; 2 mg/ml, max 4 min), the neurolemma was partially digested and the main tracheal branches and fat body were removed. The protease was rinsed off carefully and replaced by Ringer solution. A saline jet was generated with a Ringer-filled electrode to remove the extracellular matrix and to expose the HS cell somata for recording.

Genetically labeled green fluorescent HS cell somata were approached with a patch electrode filled with a red fluorescent dye (intracellular solution; Wilson and Laurent 2005) containing an additional 5 mM Spermine (S-2876, Sigma–Aldrich) and 30 mM Alexa Fluor 568–hydrazide-Na (A-10441, Molecular Probes) adjusted to pH = 7.3). Recordings were established under visual control with a ×40 water-immersion objective (LumplanF, Olympus), a Zeiss microscope (Axiotech Vario 100, Zeiss, Oberkochen, Germany), fluorescence excitation (100-W fluorescence lamp, heat filter, neutral-density filter OD 0.3; all from Zeiss), and a dual-band filter set (EGFP/DsRed, Chroma Technology, Bellows FallsVT). During the recordings, the fluorescence excitation was shut off to prevent blinding of the fly. Patch electrodes of 6- to 8-MΩ resistance (thin wall, filament, 1.5 mm; WPI, Sarasota, FL) were pulled on a Sutter- P97 (Sutter Instrument, Novato, CA). A reference electrode (Ag-AgCl) was immersed in the extracellular saline (pH 7.3, 1.5 mM $CaCl_2$, no sucrose). Signals were recorded on a BA-1S Bridge Amplifier (npi electronics, Tamm, Germany), low-pass filtered at 3 kHz, and digitized at 10 kHz via a D/A converter (PCI-DAS6025, Measurement Computing, Norton, MA) with Matlab (version 7.3.0.267, The MathWorks, Natick, MA). After the recording, several images of each Alexa-filled LPTC were taken at different depths along the *z*-axis (HQ-filter set Alexa-568, Chroma Technology) with a charge-coupled device (CCD) camera (Spot Pursuit 1.4 Megapixel; Visitron Systems, Puchheim, Germany).

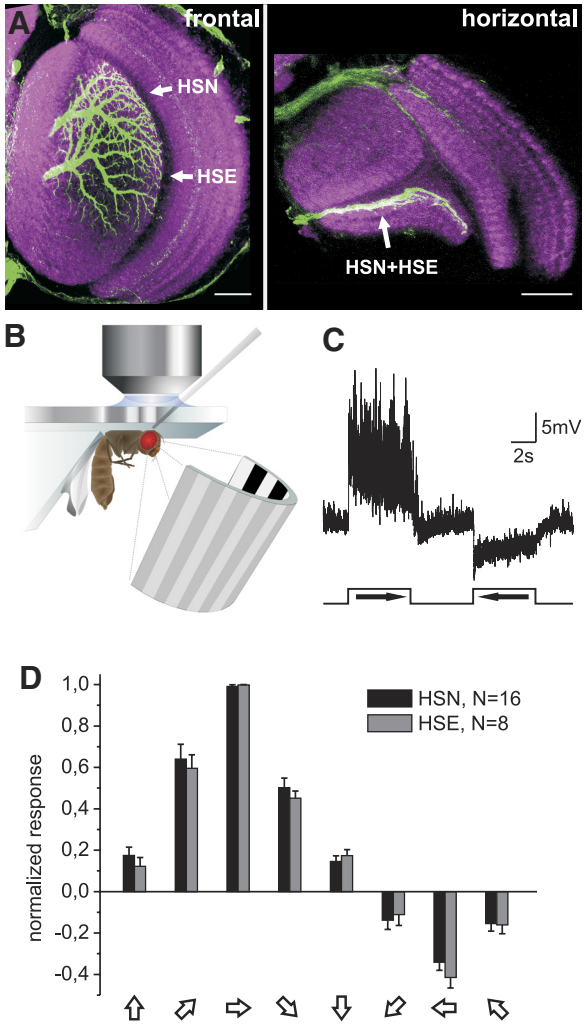

FIG. 1. Basic anatomy and response properties of horizontal system (HS) cells in *Drosophila*. *A*: the Gal4-line NP0282 drives expression of the fluorescent marker mCD8–green fluorescent protein (GFP) in 2 neurons of the lobula plate. Based on their anatomy and on comparable neurons in large dipteran flies these neurons were previously described as the northern (HSN) and equatorial (HSE) cells of the *Drosophila* HS system. Their dendrites cover large overlapping areas (frontal section) in a thin anterior layer (horizontal section) of the lobula plate. For whole cell recordings from these neurons only their somata were fluorescently labeled (see METHODS). Scale bars: 25 μm. *B*: scheme of the recording setup and preparation of the fly under the fluorescence microscope. In the lower dry half of the preparation the fly is looking at moving patterns presented on a light-emitting diode arena. *C*: canonical response of an HSN cell plotted against time. A vertical sine grating (λ = 42.5°) moving horizontally (temporal frequency = 1 Hz) elicits a directionally selective response. Large-field rotation with an ipsilateral front-to-back component (preferred direction [PD]) elicits a strong depolarization. Motion in the opposite direction (null direction [ND]) elicits a strong hyperpolarization of the membrane potential. Small, fast membrane fluctuations increase in size during PD motion. *D*: directional tuning. Plotted is the mean response amplitude during 5-s grating motion (same stimulus as in *C*) in 4 different orientations and a total of 8 different directions. HSN and HSE respond strongest to horizontal motion. Error bars indicate SE.

Immunohistochemistry

Female flies were dissected 3 to 5 days after eclosion. Their brains were removed and fixed in 4% paraformaldehyde for 30 min at room temperature. Subsequently, the brains were washed for 45–60 min in PBT [phosphate-buffered saline (pH 7.2) including 1% Triton X-100]. For antibody staining, the samples were incubated in PBT including 2% normal goat serum (Sigma–Aldrich, G9023) for 1 h at room

temperature followed by incubation with primary antibodies (1:200, overnight at 4°C). Primary antibodies were removed by several washing steps (5 × 20 min in PBT) and secondary antibodies were added (1:200, overnight at 4°C). The samples were further washed with PBT (3 × 20 min) followed by final washing steps in PBS (3 × 20 min). The stained brains were mounted in Vectashield (Vector Laboratories, Burlingame, CA) and analyzed by confocal microscopy (see following text). The following primary and secondary antibodies were used: Alexa Fluor 488 rabbit anti-GFP-IgG (A-21311, Molecular Probes), mouse anti-Dlg (4F3, Developmental Studies Hybridoma Bank), and Alexa Fluor 594 goat anti-mouse IgG (A11005, Molecular Probes).

Intracellular dye filling

Flies expressing mCD8-GFP driven by G73 were decapitated. The cut heads were fixed in a layer of two-component glue (UHU Plus; UHU, Baden, Germany), with the compound eyes looking downward into the glue. After hardening of the glue (~2 min) the specimen were covered with Ringer solution and the cuticle at the back side of the fly's head was removed with sharp needles (Neolus, Gx3/4 in. 0.4 × 20 mm). This procedure allowed direct access to the brain. The main tracheal branches were removed. Dye fillings were performed using quartz electrodes (QF 100-60-10; Sutter Instrument) pulled on a laser puller (P-2000; Sutter Instrument). Electrodes were filled with a 10 mM Alexa Fluor 594 solution (A10442; Invitrogen, Karlsruhe, Germany) and backfilled with 2 M KAc/0.5 M KCl solution. Impaled cells were loaded by negative current pulses for a few seconds. Subsequently, the brains were fixed in 4% paraformaldehyde for 15 min.

Confocal microscopy and reconstruction

Serial optical sections were taken at 0.5 μm intervals with 1024 x 1024 pixel resolution using confocal microscopes (Leica TCSNT) and oil-immersion ×40 (numerical aperture [NA] = 1.25) or ×63 (NA = 1.4) Plan-Apochromat objectives. The individual confocal stacks were analyzed using Image J (National Institutes of Health, Bethesda, MD) software. The size, contrast, and brightness of the resulting images were adjusted with Photoshop CS (Adobe Systems, San Jose, CA).

Cells were manually traced using previously described custom-written software (Cuntz et al. 2008), resulting in detailed cylinder models. Lobula plate volumes were reconstructed manually by outlining their outer borders in each slice and sampling surface meshes. Cylinder and volume models were visualized using the Blender animation system (http://www.blender.org).

Neurobiotin staining

HS cells were targeted and perfused with patch electrodes as described earlier. Neurobiotin (2–4%; Vector Labs) was added to the intracellular solution. Neurobiotin and Alexa Fluor 568 were coinjected via ±0.2-nA current pulses for ≤10 min. For initial identification, the perfused individual HS cell was imaged with the fluorescence microscope and CCD camera as described earlier. Staining against Neurobiotin with Streptavidin–Alexa Fluor 568 conjugate (1:100, Invitrogen) was performed as described earlier, except that whole fly heads were fixed in 4% paraformaldehyde (2 h) before dissection in PBS. Perfusion of a single HS cell never resulted in more than one Alexa Fluor 568–filled cell. Only after labeling of Neurobiotin with Streptavidin–Alexa Fluor 568 conjugate did other cells light up. The second red label was used to prevent spectral overlap with the green fluorescence of genetically labeled neurons.

Visual stimulation

For visual stimulation a custom-built light-emitting diode (LED) arena was used based on the open-source information of the Dickinson Laboratory (http://www.dickinson.caltech.edu/PanelsPage). Our arena consists of 15 × 8 TA08-81GWA dot matrix displays (Kingbright, Walnut, CA), each harboring 8 × 8 individual green (568-nm) LEDs, covering 170° in azimuth and 85° in elevation of the fly's visual field, with an angular resolution of about 1.4° between adjacent LEDs. The arena is capable of frame rates above 600 frames/s, with 16 intensity levels. To measure the velocity tuning, patterns were generated in which four consecutive frames were used to define one image. This resulted in 64 equidistant intensity levels available per pixel. Each dot matrix display is controlled by an ATmega644 microcontroller (Atmel, San Jose, CA) that obtains pattern information from one central ATmega128-based main controller board, which in turn reads in pattern information from a compact flash memory card. For achieving high frame rates with a system of this size, each panel controller was equipped with an external AT45DB041B flash memory chip for local pattern buffering. Matlab was used for programming and generation of the patterns as well as for sending the serial command sequences via RS-232 to the main controller board and local buffering. The luminance range of the stimuli was 0–8 cd/m^2.

Large-field stimuli covered the whole extent of the arena. To study direction selectivity, sine gratings of four different orientations (spatial wavelength: 42.5° for the horizontal, 45° for the vertical, and 32° for the diagonal patterns) moving in eight different directions at a temporal frequency of 1 Hz were presented.

For the velocity tuning, two sine gratings of either 22.4 or 44.8° spatial wavelength were presented moving at nine different angular velocities corresponding to temporal frequencies of 0.1 to 5 Hz. The sequence of velocities was changed during experiments.

To study contrast dependence, a square-wave grating of 34° spatial wavelength moved at a constant angular velocity of 34°/s, corresponding to a temporal frequency of 1 Hz. Contrast was calculated as $(I_{max} - I_{min})/(I_{max} + I_{min})$. With the 16 intensity levels of the LEDs, seven pattern contrasts could be obtained ranging from 100% to 6.7% at the same mean luminance. To obtain a lower contrast of 3.3%, four consecutive image frames were used to define one image as described earlier.

The square-wave grating (spatial wavelength: 22.4°; angular velocity: 22.4°/s) used for either ispilateral or contralateral stimulation covered about 56° in azimuth and 85° in elevation and was displaced by ±15° relative to frontal gaze.

The local response characteristics of HS cells were determined using a previously described stimulus (Nordström et al. 2008; Wertz et al. 2009). A small bar of 5.6° length and 1.4° width was moved horizontally from the contra- to the ipsilateral side and back again at different elevations or vertically downward and upward at different positions along the azimuth. For both the vertical and horizontal stimuli an area of about 145° along the azimuth and 85° of elevation was covered. A typical response trace for the horizontal and the vertical local stimulus is shown in Supplemental Fig. S2.[1]

Data analysis

Data were acquired and analyzed with the data acquisition and analysis toolboxes of Matlab. Receptive fields were calculated by binning the responses of single HS cells to horizontal stimulation (~5.6° elevation and ~5.6° azimuth) and subtracting the mean response during null direction from the mean response during preferred direction (PD) motion. The receptive fields of all HS cells of a certain type were averaged, smoothed by convolving them with a 3 × 3 kernel approximating an isotropic Gaussian function, and normalized to maximal value.

The horizontal and vertical sensitivity components for the vector fields were calculated locally and used to calculate a single local vector for each region that results in the shown vector fields. Importantly, it was recently shown that these x- and y-components are fully

[1] The online version of this article contains supplemental data.

sufficient to determine the local orientation tuning and directional preference of the cell (Wertz et al. 2009).

To analyze the velocity dependence the mean response of the first 500 ms after the onset of PD motion was taken. In all other cases the mean over the whole stimulus duration was calculated. The mean potential during 500 ms before stimulus onset was used as a baseline and subtracted from this response.

RESULTS

Based on anatomical similarity to the three horizontally sensitive LPTCs in blowflies (Hausen 1982a,b), the horizontal system of *Drosophila* has been proposed to consist of the three giant output neurons HSN, HSE, and HSS (Fischbach and Dittrich 1989; Heisenberg et al. 1978). The dendrites of these cells reside in a thin anterior layer of the lobula plate (Fig. 1*A*), where they cover the dorsal, middle, and ventral parts of this retinotopically organized neuropile, respectively (Heisenberg et al. 1978; Scott et al. 2002). Their axons project centrally to the lateral protocerebrum, where they are supposed to synapse onto descending neurons (Eckert and Meller 1981; Haag et al. 2007) and thus to control optomotor turning responses induced by horizontal optic flow.

We performed in vivo whole cell recordings from the somata of HS cells and characterized their response properties during large-field visual motion (Fig. 1*B*). In the first series of experiments reproducible recordings from identified cells were enabled using the NP 0282 Gal4 driver line. At the level of the lobula plate, NP 0282 specifically labels HSN and HSE (Fig. 1*A*). Despite the lack of HSS, NP 0282 was chosen to express a green fluorescent marker that highlights the soma (Joesch et al. 2008) of HSN and HSE under the fluorescence microscope. The recording electrode was visualized by adding a red fluorescent dye to the electrode solution, which allowed directing the electrode under visual guidance toward the green cell bodies. During the recording, the cells became perfused with the red dye and the recorded signals could be assigned to the specific cell type. In these recordings, HS cells exhibited a resting membrane potential of about −55 mV (corrected for liquid junction potential) and an input resistance of 100–200 MΩ ($n = 25$). At rest, all recorded HS cells showed small and rapid spontaneous membrane fluctuations of high frequency (Fig. 1*C*).

HSN and HSE are tuned to horizontal motion in a direction-selective way

When stimulated with a large-field sine grating (spatial wavelength = 42.5°) moving front-to-back in front of the ipsilateral eye (including an area of back-to-front motion in the contralateral eye), HS cells canonically exhibited a graded depolarization superimposed by spikelike events (Fig. 1*C*). Motion in the opposite direction led to a hyperpolarization of the membrane potential and a reduction of the fast spikelike events. Presentation of sine gratings moving in four different orientations and a total of eight different directions revealed a strong directional tuning of both HSN and HSE (black and gray bars, respectively, Fig. 1*D*) to large-field horizontal motion, similar to their counterparts in *Calliphora.* Ipsilateral front-to-back motion elicited the strongest activation (preferred direction [PD]) and back-to-front motion the strongest inhibition (null direction [ND]). Typically, ND responses were smaller in amplitude than PD responses. Diagonal motion led to weaker responses and almost no responses were elicited by vertical motion in either direction. Thus HS cells in *Drosophila* are tuned to large-field horizontal motion in a directional-selective way.

HS cell responses suggest input from correlation-type motion detectors

According to the correlation-type model for elementary motion detection (Borst and Egelhaaf 1989; Reichardt 1961), motion information is extracted from the retinal image by a multiplicative interaction of luminance signals from two neighboring receptors after delaying one of them in time. Large-field directional selectivity of LPTCs can then arise from spatial integration of input from two arrays of such detectors, one excitatory and the other inhibitory, that compute local motion information with opposite preferred direction (Joesch et al. 2008; Raghu et al. 2007, 2009; Single and Borst 1998; Single et al. 1997). The output of such a correlation-type model has certain features that we tested for in HS cell responses. These features are the appearance of a velocity optimum (Reichardt 1961) (Fig. 2*A*), the linear dependence of this velocity optimum on the spatial wavelength of the moving grating (Fig. 2*B*), the dependence of the response on the magnitude of contrast (Buchner 1984) (Fig. 2*C*), and the independence of the sign of contrast (Egelhaaf and Borst 1992) (Fig. 2*D*). To characterize the velocity dependence of HS cells in response to PD motion, we presented sine gratings of 22 or 44° spatial wavelength (Fig. 2*A*, *inset*) at nine different velocities (Fig. 2*A*). For both patterns the HS cell response increased nonlinearly, exhibited a maximum response at an angular velocity of 22 and 44°/s, respectively, and declined at higher velocities (Fig. 2*A*). For both patterns this resulted in a maximal response at around 1 Hz (velocity [deg/s] divided by spatial wavelength [deg]), which represents the so-called temporal frequency optimum, a hallmark of the correlation-type detector model (Fig. 2*B*).

The dependence of the response on the magnitude of contrast was shown by presenting square-wave gratings (spatial wavelength: 34°) of different contrasts, ranging from 3.3 to 100%, that were moving at a constant velocity of 34°/s (Fig. 1*C*). For both PD and ND motion the response amplitudes increased with pattern contrast and PD responses saturated at higher contrast (Fig. 2*C*). Furthermore, the correlation-type motion detector reports the direction of movement independent of the sign of contrast. In accordance with this prediction, a moving dark bar on a light background or a moving light bar on a dark background evoked depolarizing PD responses for front-to-back motion and hyperpolarizing ND responses for back-to-front motion (Fig. 2*D*). In these experiments a still bar was presented to the contralateral field of view, began to move at time *a*, entered the ipsilateral field of view at time *b*, continued its way and stopped at a lateral position at time *c*. From there it moved back by reversing the sequence *c′*, *b′*, and *a′* (Fig. 2*D*). Regressive motion of the bar through the contralateral visual field of view elicited a depolarizing response, although it was smaller than that caused by ipsilateral progressive motion (see following text). Taken together, the response properties of HS cells are indicative of presynaptic computations according to the correlation-type model of motion detection.

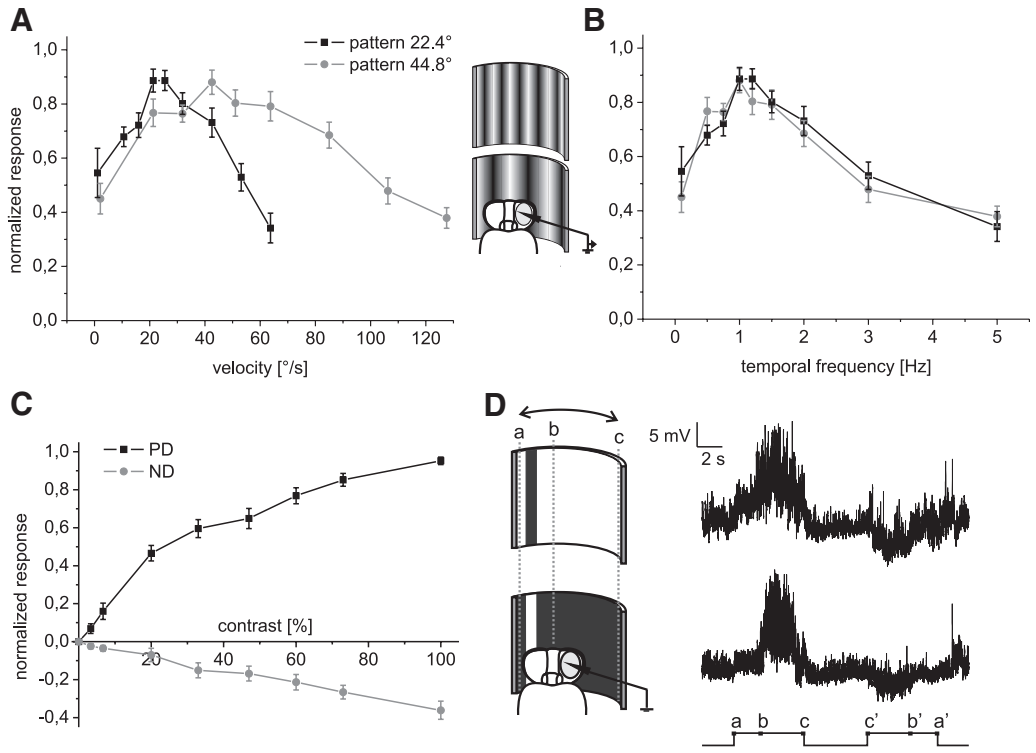

FIG. 2. HSN and HSE responses match the predictions of a correlation-type motion detector. *A*: velocity dependence. Two sine gratings of different spatial wavelength ($\lambda = 22.4°$, $\lambda = 44.8°$) moving at 9 different velocities elicited a velocity optimum that depended on the spatial wavelength of the pattern. Plotted is the mean response during the first 500 ms after onset of PD motion, normalized to the maximal response for each fly ($n = 10$ for each grating; error bar: SE). *B*: constant temporal frequency optimum of 1 Hz. Same data as in *A* plotted against the temporal frequency (tf = velocity/λ). *C*: contrast dependence. Square-wave gratings ($\lambda = 34°$) of different contrast moving in PD or ND (tf = 1 Hz) were presented. Plotted is the mean response during 5 s of motion normalized to the maximal response of each HS cell. Response amplitudes increase with contrast, but exhibit saturation ($n = 19$; error bars: SE). *D*: independence of the sign of contrast. Example trace of an HS cell responding to a light bar on a dark background and a dark bar on a light background moving in PD and ND (width of the bar: 8.5°, maximal contrast). The direction of motion is reported by the membrane potential independent of the sign of contrast. *a*, *b*, and *c* and *a′*, *b′*, and *c′* mark the time points at which the bar occupied the respective positions on the arena (see *inset*). Note that HS cells respond to motion on the contralateral side (*a* to *b* and *b′* to *a′*) as well. Ipsilateral motion elicited stronger responses (*b* to *c* and *c′* to *b′*).

HS cells of one hemisphere have strongly overlapping, binocular receptive fields

The environment, as scanned by the ipsilateral compound eye, is mapped retinotopically onto the columnar elements that are supposed to provide the synaptic input to the giant HS cell dendrites in the lobula plate (Braitenberg 1970; Strausfeld 1984). As a consequence of this layout, the position and the branching pattern of an HS cell within the lobula plate (Fig. 3*A*) should be predictive of its ipsilateral receptive field (Hausen 1982a,b). To analyze the dendritic structure of all three HS cells in detail we filled HSS of one hemisphere with a red fluorescent dye in three flies, in which HSN and HSE were labeled with green fluorescent protein (GFP), and reconstructed their dendritic trees from confocal image stacks (Supplemental Fig. S1, Fig. 3*A*). The dendrites of HSN, HSE, and HSS cover dorsal, equatorial, and ventral parts of the lobula plate, where they occupy on average 70, 90, and 75% of the total area, respectively. The overlap of their dendritic spanning fields is extremely large (Fig. 3*B*); HSE covers about 90% of HSN and about 80% of HSS. A dendritic branch of HSE reaches close to the dorsalmost boundary of HSN (Fig. 3*A*). Even HSN and HSS dendrites overlap to about 20%. Any deviation of the receptive field from this anatomical map can possibly be attributed to input from neurons other than the columnar ones.

In the course of our experiments we occasionally recorded from genetically unlabeled HS cells in different genotypes that represented control situations and identified the recorded cells by filling them with the red fluorescent dye of the electrode solution. The recordings of these cells were indistinguishable from our previous recordings of genetically labeled HSE and HSN and included recordings from HSS cells that were not highlighted by the Gal4-driver in the previous experiments. We analyzed the receptive fields of genetically labeled and unlabeled HSN, HSE, and HSS cells, respectively, by presenting a small vertical bar (5.6° high and 1.4° wide) moving horizontally at different positions subtending 145° along the azimuth and about 85° of elevation (see METHODS; Nordström et al. 2008; Wertz et al. 2009). A typical response trace recorded during such an experiment is shown in Supplemental Fig. S2. The relatively large membrane potential fluctuations in response to this local motion stimulus suggest a rather unexpected (Borst and Haag 1996) short electrotonic distance from the dendrite to the recorded soma or, alternatively, active processes that enhance signal propagation (Gouwens and Wilson 2009). However, these results and the presence of small excitatory postsynaptic potentials in all recordings suggest that even potential unitary events propagate well to the soma.

We binned the response within a time window that corresponded to motion of about 5.6° along the azimuth and plotted

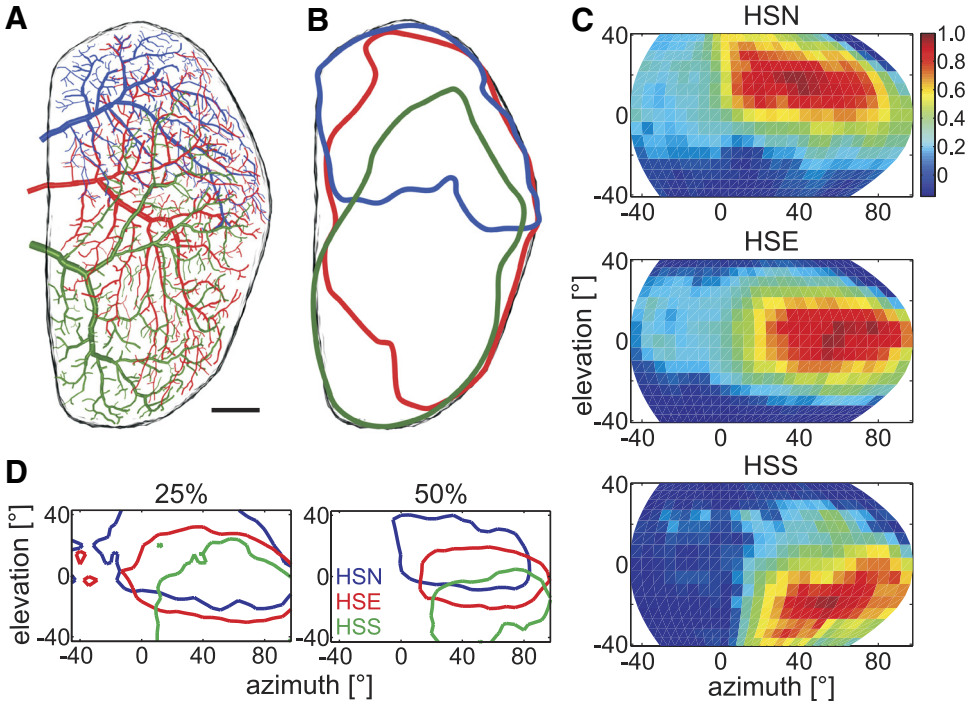

FIG. 3. Dendritic structure and receptive fields of HSN, HSE, and HSS. *A*: reconstruction of the dendritic arborization of HSN (blue), HSE (red), and HSS (green) in the lobula plate from confocal image stacks (HSN and HSE were GFP-labeled and HSS was filled with Alexa Fluor 594). Scale bar: 20 μm. *B*: outline of the dendritic spanning field of HSN (blue), HSE (red), and HSS (green) from *A*. In particular the spanning fields of HSE and HSS cover large parts of the lobula plate and the dendrites of all 3 HS cell dendrites overlap extensively. *C*: receptive fields of HSN, HSE, and HSS. Plotted are response amplitudes (PD–ND) elicited by a small bar moving horizontally at different elevations normalized to the maximal response. HSN, HSE, and HSS are most responsive to motion at positions covered by their own dendritic trees in the lobula plate (that is more dorsal for HSN, equatorial for HSE, and more ventral for HSS). HSN and HSE additionally respond to contralateral motion. All HSS responses were recorded from cells ($n = 5$) without GFP expression and all HSN responses from genetically labeled cells ($n = 7$). Data for HSE are from unlabeled ($n = 4$) and GFP-labeled ($n = 4$) cells. *D*: overlap of the receptive fields. The amount of overlap between the receptive fields of HSN (blue), HSE (red), and HSS (green) was estimated by applying a threshold of 50 or 25% of the maximal response in *C*. For both thresholds the receptive fields of all 3 HS cells intersect in the equatorial area. Compare with the overlap of the dendritic trees in *B*.

the normalized response amplitudes (PD − ND) in false color code against the position of the bar on the arena (Fig. 3*C*). Because the arena is curved only in the horizontal direction, the size of the bar as stated earlier is valid for only the equatorial position and appeared slightly smaller to the fly in the dorsal and ventral parts of the visual field. Our analysis revealed that HSN, HSE, and HSS cells in *Drosophila* have large receptive fields that cover at their largest extent over 60° of elevation. HS cells are most sensitive to motion at positions corresponding to their dendritic trees in the lobula plate, which is dorsal for HSN, equatorial for HSE, and ventral for HSS (Fig. 3, *A* and *C*). In contrast to *Calliphora* (Hausen 1982b), however, HSE in *Drosophila* seems to be maximally sensitive in the lateral visual field and not in the frontal one.

To estimate the amount of overlap between the receptive fields of HSN, HSE, and HSS, a threshold of either 25 or 50% of the maximal response was set. The areas where the responses of HSN, HSE, or HSS exceeded the threshold were encircled in blue, red, and green, respectively (Fig. 3*D*). If a threshold of 25% is used, the receptive fields of HSN and HSS overlap strongly with that of HSE. The receptive field of HSN reaches almost as far ventrally as that of HSE and that of HSS nearly as far dorsally as that of HSE. In an equatorial area extending ≤40° in the dorsoventral axis the receptive fields of all three HS cells overlap. Even if a threshold of 50% is used, there is a small equatorial region where the receptive fields of all three HS cells intersect. The huge overlap of the receptive fields of HSN, HSE, and HSS corresponds in part to the overlap of their dendrites stated earlier. However, the dorsoventral extension of the receptive field of HSE seems to be somewhat smaller than expected from its dendritic spanning field (compare Fig. 3, *B*, *C*, and *D*). One explanation might be that we miss signals from remote dendrites due to recording from the soma and thus underestimate the size of the receptive field. In contrast, the lack of dendritic branches of HSN in the ventral area indicates that the ventral extension of the receptive field of HSN cannot be explained by direct input to the dendrite alone (compare Fig. 3, *B* and *D*).

Another interesting feature of the receptive fields of HSN and HSE is their sensitivity to contralateral motion (Hausen 1982a; Krapp et al. 2001) (Fig. 4). We presented moving square-wave gratings in either the ipsilateral or the contralateral part of the visual field to investigate this in further detail. The pattern covered about 56° in azimuth and 85° in elevation. To prevent stimulation of the area of binocular overlap, which consists of three vertical rows of ommatidia (Heisenberg and Wolf 1984), the pattern was displaced by ±15° with respect to the frontal gaze of the fly (Fig. 4). Motion in front of the ipsilateral eye elicited canonical PD and ND responses i.e., a depolarization for front-to-back and a hyperpolarization for back-to-front motion. Contralateral back-to-front motion, however, elicited a robust depolarization, whereas contralateral front-to-back motion did not elicit a noticeable response. Thus HSN and HSE are tuned to rotational panoramic motion stimuli

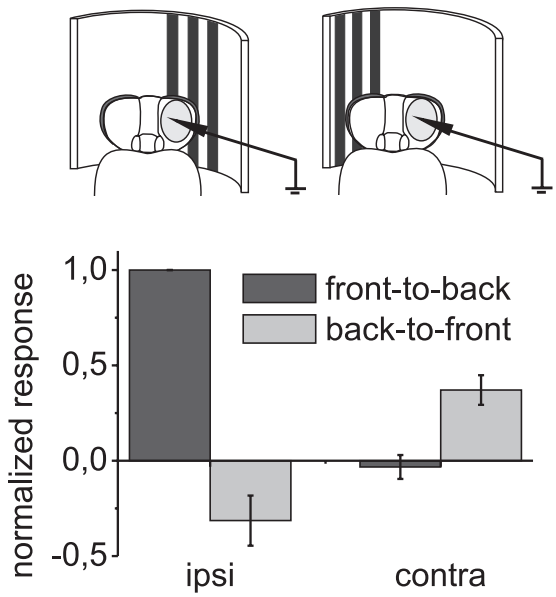

FIG. 4. Sensitivity to contralateral motion. Square-wave gratings (λ = 22.4°) were presented in either the contra- or the ipsilateral visual field as shown in the schematic drawing (sparing the frontal region of binocular overlap). Contralateral back-to-front motion elicited a weak depolarization of the membrane potential in HS cells and a strong depolarization in response to ipsilateral front-to-back motion (n = 6; error bar: SE).

as they arise from rotation of the animal around the vertical body axis. Importantly, their sensory input is not confined to the retinotopically organized columnar neurons that impinge onto their dendritic tree.

We characterized the receptive fields in further detail by presenting a local bar moving vertically in addition to the horizontally moving bar as shown earlier (see METHODS; Nordström et al. 2008; Wertz et al. 2009). From the responses to local horizontal and vertical motion, we calculated response vectors that indicate by their orientation the local preferred direction and by their length, the strength of the response. Motion vectors calculated this way were recently shown to be identical to resulting motion vectors calculated from periodic gratings that drifted in many different orientations and directions (Wertz et al. 2009). All local vectors together constitute the optic flow field of a given HS cell (Fig. 5). All three HS cells exhibited a slight vertical sensitivity. HSN (Fig. 5*A*) and, to a weaker extent HSE (Fig. 5*B*), depolarize in response to upward motion in the frontodorsal and frontoequatorial parts of their receptive fields. HSS shows a similar sensitivity to upward motion in a more ventrolateral position (Fig. 5*C*).

Dye-coupling suggests that HS cells are part of a network of electrically coupled neurons

In *Calliphora*, complex receptive fields of VS and HS cells arise from electric coupling to other LPTCs and descending neurons (Cuntz et al. 2007; Haag and Borst 2004). Injection of Neurobiotin, a molecule sufficiently small to pass Innexin-based gap junctions, and double recording revealed that neurons that allow the spread of Neurobiotin are indeed electrically coupled in *Calliphora* (Haag and Borst 2005).

We investigated whether this also holds true for HS cells in *Drosophila.* For that purpose, Neurobiotin was added to the intracellular solution in the recording electrode. GFP-labeled HSN or HSE cells were filled via their somata. We used patch electrodes instead of sharp electrodes to avoid unspecific labeling that might be caused by brief penetration of other neurons. Perfusion with Alexa-568 allowed for immediate identification of the recorded neuron. Later, the spread of Neurobiotin was detected by staining with Streptavidin-coupled Alexa-568 (Joesch et al. 2008). Because the initially perfused free Alexa-568 never stained other cells except the injected one, we concluded that fluorescence after Streptavidin–Alexa-568 labeling in other cells is due to direct or indirect coupling via electrical synapses to the recorded cell (Fig. 6).

When we injected Neurobiotin into either HSN (Fig. 6, *A* and *B*) or HSE (Fig. 6*C*), one or both of the remaining

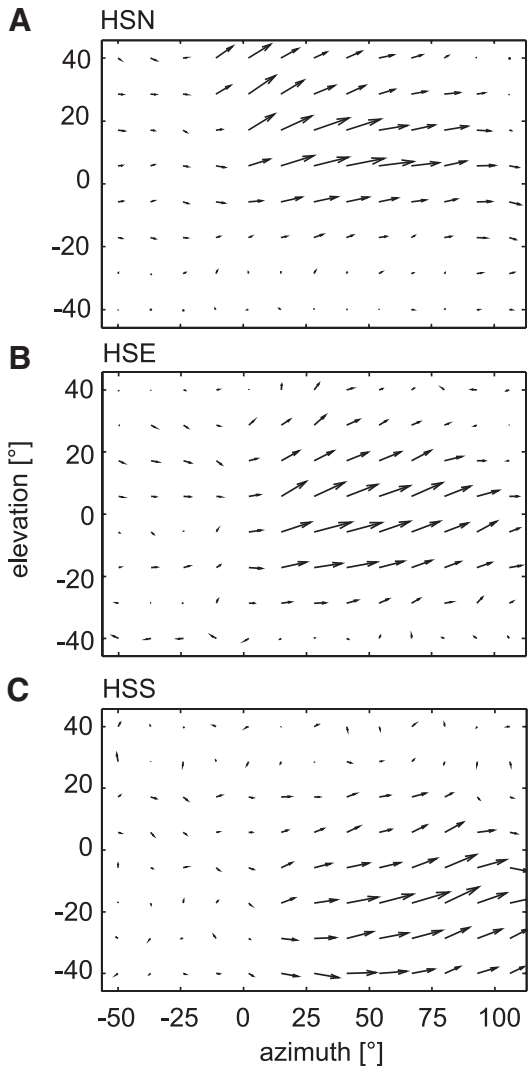

FIG. 5. Vector fields of HSN (*A*), HSE (*B*), and HSS (*C*). Local preferred direction and response strength of all 3 HS cells are indicated by the orientation and lengths of the motion vectors (arrows). Vectors were calculated by subtracting PD and ND responses to small bars moving either horizontally or vertically at different positions (compare Fig. 3). Similar to HSN and HSE the maximum sensitivity in the ventral receptive field of HSS corresponds to the area occupied by its dendritic tree in the lobula plate (not shown). As the other HS cells, HSS responds mainly to horizontal motion. However, all HS cells show a slight sensitivity to upward motion in mostly the center of their receptive field. All responses from HSS (n = 6) and HSE (n = 9) were recorded from unlabeled cells. HSN vector maps were calculated from the local responses of labeled (n = 4) and unlabeled cells (n = 1).

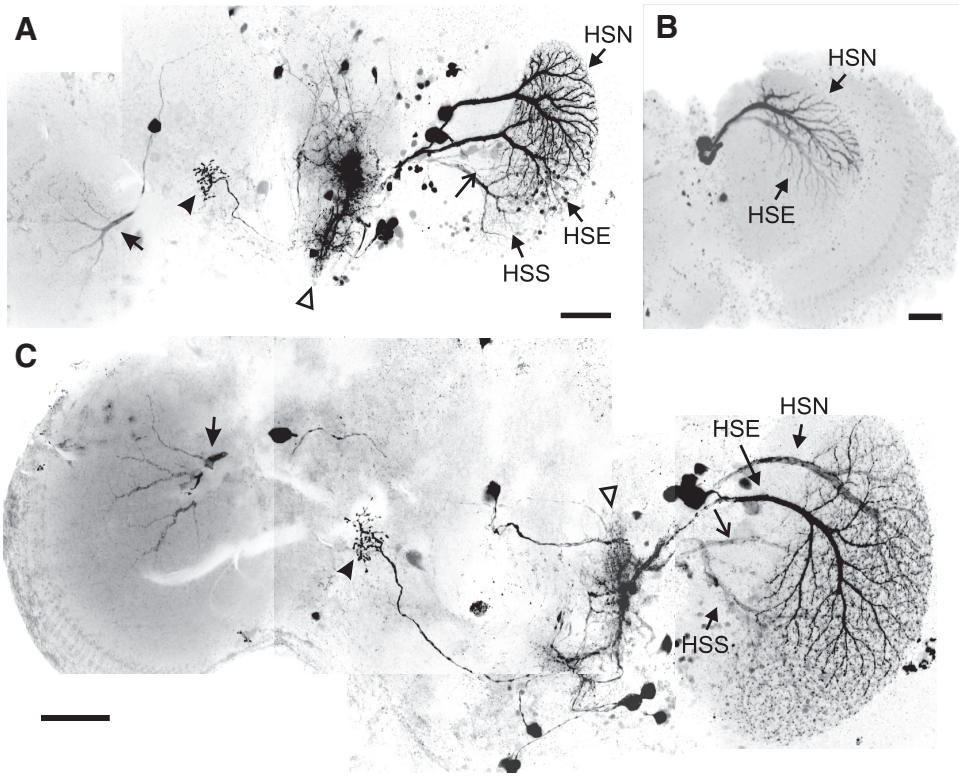

FIG. 6. Spread of Neurobiotin within the HS circuitry. The spread of Neurobiotin, which can pass through Innexin junctions, provides indirect evidence for electric coupling among HS and other cells. Neurobiotin was injected into either HSN (*A* and *B*) or HSE (*C*) and visualized with Streptavidin coupled to a red fluorescent dye. Costaining was detected in neighboring HS cells (named in *A* to *C*), unidentified ipsilateral descending neurons (open triangle), cells projecting to the contralateral protocerebrum where HS cell axons terminate (arrowheads in *A* and *C*), contralateral lobula plate tangential cells (LPTCs; filled arrows in *A* and *C*), and occasionally in unidentified fibers in the same lobula plate (open arrows in *A* and *C*). The figure shows composite images of maximum intensity projections of confocal image stacks taken from neighboring regions of the brain. Scale bars: 50 μm.

ipsilateral HS cells were typically labeled. In contrast to similar experiments in *Calliphora*, no CH cells were found to be colabeled (Haag and Borst 2005). From this observation we conclude that HS cells in *Drosophila* are directly or indirectly coupled with each other. Nevertheless, we observed additional staining in fibers other than the three HS cells in the same lobula plate (Fig. 6, *A* and *C*). Unfortunately, the staining was too weak to enable unequivocal identification of these processes. In these cases the arborization of an LPTC in the contralateral lobula plate was also labeled (filled arrows in Fig. 6, *A* and *C*) that might belong to the unidentified ipsilateral processes mentioned earlier. This cell represents a likely candidate neuron to provide contralateral input to HS cells (Figs. 2, 3, and 4). In addition, HS cells were extensively dye-coupled to descending neurons (open triangles in Fig. 6, *A* and *C*) that could not be identified individually. One frequently labeled neuron has a prominent arborization on the contralateral side and probably connects the output region of HS cells of both hemispheres (arrowhead in Fig. 6, *A* and *C*). Taken together, our findings suggest that HS cells are part of a complicated network of electrically coupled neurons. This network comprises descending neurons, ipsilateral HS cells, and LPTCs from the same and the contralateral hemisphere so far unidentified in *Drosophila*. The columnar input to the ipsilateral dendrite and the electric coupling to the LPTC network are likely sufficient to account for the wide receptive fields and rotational tuning of HS cells.

DISCUSSION

Drosophila reacts to horizontally drifting retinal images with compensatory yaw-torque responses to stabilize straight-flight segments (Heisenberg and Wolf 1984). The giant HS cells in the lobula plate are thought to play a key role in the control of this behavior, although their exact role remains elusive. Patch-clamp recordings in *Drosophila* were only established recently (Wilson et al. 2004) and physiological data from *Drosophila* HS cells were not available so far. We used the Gal4/UAS-system (Brand and Perrimon 1993) to fluorescently label two of the three HS cells, HSN and HSE, which allowed for the investigation of their basic anatomy (Figs. 1 and 3) and targeting for reliable recordings from their somata (Figs. 1–3); neighboring HSS cells were recorded and filled without the use of genetic labeling (Figs. 3 and 5). In *Drosophila*, whole cell recordings are so far feasible only from the soma. They allow for reliable and stable recordings for $\leq$1 h. We describe the response characteristics of all three giant neurons of the HS system in *Drosophila*, their directional selective output, receptive field organization, and network interactions.

Basic response properties of Drosophila HS cells

Concerning their basic response properties, we found that HS cells in *Drosophila* are largely similar to their counterparts in *Calliphora* (Hausen 1982a,b). They respond to horizontal motion with graded membrane potential changes in a directional-selective way (Fig. 1). Their responses are indicative of input from elementary motion detectors of the correlation type (Fig. 2) because they are independent of the sign of contrast and exhibit a velocity optimum that linearly depends on the spatial wavelength of the moving periodic grating. Such a dependence results in a single temporal frequency optimum and is a characteristic feature of presynaptic computations according to the correlation-type detector model (Borst and Egelhaaf 1989; Reichardt 1961). The temporal frequency optimum of 1 Hz (Fig. 2*B*) precisely matches the results from our

previous account on *Drosophila* VS cells (Joesch et al. 2008) and findings from H1 cells in *Calliphora* (Haag et al. 2004). However, recordings from HS cells in *Calliphora* resulted in higher values of 2–5 Hz (Hausen 1982b), suggesting slight differences between the two fly species. The quadratic dependence of the response on the contrast predicted by a correlation-type detector model is generally found only in the low-contrast range (Buchner 1984). However, a detailed and satisfying analysis of the low-contrast regime cannot be performed using our LED arena. At higher contrasts, the responses saturate (Fig. 2*C*), probably due to a gain control mechanism in elementary motion detectors. The cellular implementation of these motion detectors is still an open question in the field.

Anatomical layout of HS cell dendrites and receptive fields

The image of the environment is represented by retinotopically organized columnar maps in the optic lobes (Braitenberg 1970; Strausfeld 1976, 1984). Within this arrangement, the dendrite of each of the HS cells occupies about 40–45% of the lobula plate in *Calliphora* (Hausen 1982a), but 70–90% in *Drosophila*. In *Calliphora*, the dendrites of HSN and HSS overlap to some extent with those of HSE, but not with each other. In *Drosophila*, in contrast, we find an area in the lobula plate, where all three cells overlap (Fig. 3*A*). Thus the overlap is much larger in *Drosophila* (Heisenberg et al. 1978) than that in *Calliphora*. In both cases female flies were studied to exclude sex-specific differences. Such differences in LPTC anatomy and number between different dipteran species have been described and were linked to differences in flight style and behavior (Buschbeck and Strausfeld 1997; Nordström et al. 2008).

The areas covered by the dendrites of HSN, HSE, and HSS correspond to the centers of large dorsal, equatorial, and ventral receptive fields, respectively. Yet, the ipsilateral receptive field of HSN significantly exceeds the area occupied by its dendrite in the lobula plate (Fig. 3). In addition, HSN and HSE are both sensitive to contralateral motion. These receptive fields of HS cells can be explained by assuming *1*) dendritic input from local motion detectors, *2*) electric coupling to neighboring HS cells, and *3*) input from contralateral neurons tuned to regressive motion. The evidence for this input organization is discussed in the following text.

IPSILATERAL COLUMNAR INPUT. The excitatory and inhibitory responses of HS cells suggest that *Drosophila* HS cells receive input from two types of elementary motion detectors with opposite preferred direction (Borst and Egelhaaf 1990; Borst et al. 1995; Single and Borst 1998). Further evidence for this scheme comes from the localization of excitatory cholinergic and inhibitory GABAergic synapses on the dendritic tips of VS and HS cells in *Drosophila* (Raghu et al. 2007, 2009) and the simultaneous integration of excitatory and inhibitory input with separate reversal potentials during grating motion (Joesch et al. 2008).

The retinotopic arrangement of the detectors is further supported by our finding that HS cells respond to local motion stimuli with a strong preference for horizontal motion. Moreover, gradual changes in local PD with a bias to upward motion were observed in the dorsofrontal (HSN and HSE) and ventrolateral (HSS) margins of the receptive field (Fig. 5). Sensitivity to vertical motion in parts of the receptive field was also reported for HS cells in *Calliphora* and was attributed to the arrangement of the ommatidial lattice in the corresponding parts of the eye (Hausen 1982b). Most likely this holds also true for *Drosophila* (Heisenberg and Wolf 1984). Neurobiotin did not spread from HS cells to vertically sensitive LPTCs in *Drosophila* (Fig. 6), although connections between HSN and lateral VS cells were reported in *Calliphora* (Haag and Borst 2005). However, in *Calliphora* these connections are supplied via the dCH cell (Haag and Borst 2007) and CH cells could not be found in *Drosophila* so far.

COUPLING TO NEIGHBORING HS CELLS. In flies, electrical connectivity schemes based on Neurobiotin coupling were previously shown to be in accordance with data obtained from double recordings (Fan et al. 2005; Haag and Borst 2005). Because our Neurobiotin injections resulted in highly reproducible patterns of stained cells, we conclude that it is a useful tool for studying direct or indirect electrical coupling. However, dye-coupling alone does not allow one to draw conclusions about the strength and functional significance of these connections.

Direct electric coupling between neighboring HS cells or via descending neurons is suggested by the spread of Neurobiotin (Fig. 6) and provides the most plausible explanation for the observed broad ipsilateral receptive field of HSN (Fig. 3). A similar ipsilateral coupling has been found in the VS cell network in *Drosophila* (Joesch et al. 2008) and within and between the HS and VS system of *Calliphora* (Farrow et al. 2005; Haag and Borst 2004, 2007). In the VS system of *Calliphora* lateral connections are thought to be responsible for the large receptive fields and thus the robustness of the response against inhomogeneous contrast distribution in the visual scene (Cuntz et al. 2007). However, HS cells in *Calliphora* are coupled to each other only indirectly via the dorsal and ventral CH cell (Cuntz et al. 2003; Haag and Borst 2002), which, by this way, receive graded input from HS cells. In response to large-field motion, CH cells in turn inhibit so-called figure-detection neurons, thereby tuning them to small-field motion (Cuntz et al. 2003; Egelhaaf 1985; Haag and Borst 2002; Warzecha et al. 1993). It is unclear how *Drosophila* solves this problem.

The fact that CH cells were never detected in our experiments matches their absence in any of the Gal4 screens and any of the detailed anatomical descriptions reported so far in *Drosophila* (Fischbach and Dittrich 1989). The weakly stained fibers next to HS cells (Fig. 6) in the ipsilateral lobula plate could not be identified due to their weak Neurobiotin labeling. The very strong and reliable coupling of HS and CH cells in *Calliphora* makes it unlikely that these weakly stained fibers represent the processes of *Drosophila* CH cells; rather, they could belong to the heterolateral projecting neurons (see following text).

INPUT FROM NEURONS WITH CONTRALATERAL RECEPTIVE FIELDS. In addition to two sources of ipsilateral input, we found sensitivity to contralateral back-to-front motion in HSN and HSE. The heterolateral projecting LPTCs detected after Neurobiotin injection (Fig. 5, *A* and *C*) are good candidates to provide this input. They might correspond to either H1 or H2, two heterolateral spiking neurons that provide input to contralateral HS cells in *Calliphora* (Haag and Borst 2001; Hausen 1982a,b;

Horstmann et al. 2000). Both cells have their dendrites in the contralateral lobula plate, where they respond to back-to-front motion with an increase in spike frequency. The axonal arborization of H1 is in the ipsilateral lobula plate. H2 axons project to the output region of HS cells in the ipsilateral protocerebrum, where they make electric contacts with HS cells. Due to the many other labeled cells and relatively weak labeling of the heterolateral neurons we could not determine whether Neurobiotin labeled H1, H2, or a third cell type. As in *Calliphora* (Götz and Buchner 1978; Hausen 1982a,b; Hausen and Wehrhahn 1989; Reichardt and Egelhaaf 1988), HSS in *Drosophila* does not respond to motion in the contralateral visual field.

Ultimately, navigation and course control in flies rely on the analysis of optic flow. Neurons that contribute to the underlying computations possess wide dendritic fields and further increase their receptive fields by connections to functionally related ipsilateral and contralateral neurons. Our data suggest that this principle is retained in the HS system of *Drosophila*, but it remains to be analyzed how the observed differences to *Calliphora* translate into differences in optomotor behavior.

Behavioral relevance

HS cells are supposed to be key players for the control of optomotor turning responses elicited by horizontal motion. This notion is mostly based on the observation that electrical responses of HS cells in *Calliphora* and optomotor torque responses in *Musca* and *Drosophila* show a similar dependence on spatial features of moving visual stimuli (Götz and Buchner 1978; Hausen 1982a,b; Hausen and Wehrhahn 1989; Reichardt and Egelhaaf 1988). In addition, elimination of the HS system in *Musca* by laser ablation (Geiger and Nässel 1981) and the *omb* mutation in *Drosophila* [largely missing HS cells and many other LPTCs and columnar neurons absent (omb; Heisenberg et al. 1978)] led to severe deficits in the execution of optomotor yaw responses.

We found that HSN and HSE in *Drosophila* are tuned to binocular rotational motion around the vertical body axis (Figs. 3 and 4). Their responses exhibit a similar dependence on features of the stimulus as optomotor yaw-torque responses, in particular a temporal frequency optimum of about 1 Hz (Fig. 2, *A* and *B*) (Buchner 1984; Götz 1964). Thus our experiments corroborate their functional contribution to compensatory turning behavior. This consent, however, is somewhat questioned by recently published behavioral experiments that report an optimum response between 5 and 10 Hz (Duistermars et al. 2007; Fry et al. 2009). At this frequency, however, HS cell responses (Fig. 2) and previously measured yaw-torque (Götz 1964) were reduced to less than half of the maximal response. It remains speculative whether this discrepancy can be attributed to differences in the stimulus presentation.

Further measurements are required to investigate whether HS cells in *Drosophila* also encode information about the structure of the visual surround during translational motion, as is suggested from experiments in blowflies (Boeddeker and Egelhaaf 2005; Kern et al. 2005). Also, lateral expansion stimuli need to be analyzed because they were reported to elicit larger optomotor responses than rotational ones (Duistermars et al. 2007; Tammero et al. 2004). In summary, HS cell output very likely feeds into multisensory neural circuits that control different behaviors of the fly (Frye and Dickinson 2001, 2004).

Concluding remarks

HS cells in *Drosophila* and large dipteran flies have largely similar response properties despite substantial differences in the organization of the neural circuitry for the detection of horizontal optic flow. Their responses are indicative of a correlation-type motion detector model. The overlap and relative size of ipsilateral HS cell dendrites are larger in *Drosophila.* CH cells, which link the HS and VS systems in *Calliphora* and are key elements of a circuitry dedicated to the detection of small moving objects, were not found in *Drosophila*. In addition, *Drosophila* HS cells exhibit a somewhat lower temporal frequency optimum than that of their counterparts in *Calliphora*. These differences might reflect adaptations to different lifestyles, given that the basic response properties of large-field motion-sensitive neurons seem to match differences in flight style (O'Carroll et al. 1996). Our functional and anatomical characterization of the HS cell circuitry in *Drosophila* can now serve to dissect *1*) the presynaptic motion detection circuitry and *2*) the exquisite control mechanism of compensatory optomotor responses by combining genetic manipulation of neuronal function with physiological recording and behavioral analysis.

ACKNOWLEDGMENTS

We thank W. Essbauer, C. Theile, and the Max Planck Institute workshop for excellent technical support; J. Plett for the design of the LED arena; R. Schorner for artwork; and J. Haag, E. Buchner, and the other members of the Borst department for discussion.

GRANTS

This work was supported by the Max-Planck-Society and by a Human Frontier Science Program grant to K. Ito, A. Borst, and B. Nelson.

REFERENCES

Boeddeker N, Egelhaaf M. A single control system for smooth and saccade-like pursuit in blowflies. *J Exp Biol* 208: 1563–1572, 2005.

Borst A, Egelhaaf M. Principles of visual motion detection. *Trends Neurosci* 12: 297–306, 1989.

Borst A, Egelhaaf M. Direction selectivity of fly motion-sensitive neurons is computed in a two-stage process. *Proc Natl Acad Sci USA* 87: 9363–9367, 1990.

Borst A, Egelhaaf M, Haag J. Mechanisms of dendritic integration underlying gain control in fly motion-sensitive interneurons. *J Comput Neurosci* 2: 5–18, 1995.

Borst A, Haag J. The intrinsic electrophysiological characteristics of fly lobula plate tangential cells. I. Passive membrane properties. *J Comput Neurosci* 3: 313–336, 1996.

Borst A, Haag J. Neural networks in the cockpit of the fly. *J Comp Physiol A* 188: 419–437, 2002.

Braitenberg V. Ordnung und Orientierung der Elemente im Sehsystem der Fliege. *Biol Cybern* 7: 235–242, 1970.

Brand AH, Perrimon N. Targeted gene expression as a means of altering cell fates and generating dominant phenotypes. *Development* 118: 401–415, 1993.

Buchner E. Behavioural analysis of spatial vision in insects. In: *Photoreception and Vision in Invertebrates*, edited by Ali MA. New York: Plenum, 1984, p. 561–621.

Buschbeck EK, Strausfeld NJ. The relevance of neural architecture to visual performance: phylogenetic conservation and variation in dipteran visual systems. *J Comp Neurol* 383: 282–304, 1997.

Chan WP, Prete F, Dickinson MH. Visual input to the efferent control system of a fly's "gyroscope." *Science* 280: 289–292, 1998.

Cuntz H, Forstner F, Haag J, Borst A. The morphological identity of insect dendrites. *PLoS Comput Biol* 4: e1000251, 2008.

Cuntz H, Haag J, Borst A. Neural image processing by dendritic networks. *Proc Natl Acad Sci USA* 100: 11082–11085, 2003.

Cuntz H, Haag J, Forstner F, Segev I, Borst A. Robust coding of flow-field parameters by axo-axonal gap junctions between fly visual interneurons. *Proc Natl Acad Sci USA* 104: 10229–10233, 2007.

Douglass JK, Strausfeld NJ. Visual motion detection circuits in flies: peripheral motion computation by identified small-field retinotopic neurons. *J Neurosci* 15: 5596–5611, 1995.

Douglass JK, Strausfeld NJ. Visual motion-detection circuits in flies: parallel direction- and non-direction-sensitive pathways between the medulla and lobula plate. *J Neurosci* 16: 4551–4562, 1996.

Douglass JK, Strausfeld NJ. Anatomical organization of retinotopic motion-sensitive pathways in the optic lobes of flies. *Microsc Res Tech* 62: 132–150, 2003.

Duistermars BJ, Chow DM, Condro M, Frye MA. The spatial, temporal and contrast properties of expansion and rotation flight optomotor responses in *Drosophila*. *J Exp Biol* 210: 3218–3227, 2007.

Eckert H, Meller K. Synaptic structures of identified, motion-sensitive interneurones in the brain of the fly, Phaenicia (Abstract). *Verh Dtsch Zool Ges* 1981: 179, 1981.

Egelhaaf M. On the neuronal basis of figure–ground discrimination by relative motion in the visual system of the fly. II. Figure-detection cells, a new class of visual interneurones. *Biol Cybern* 52: 195–209, 1985.

Egelhaaf M, Böddeker N, Kern R, Kretzberg J, Lindemann JP, Warzecha AK. Visually guided orientation in flies: case studies in computational neuroethology. *J Comp Physiol A Neuroethol Sens Neural Behav Physiol* 189: 401–409, 2003.

Egelhaaf M, Borst A. Are there separate ON and OFF channels in fly motion vision? *Vis Neurosci* 8: 151–164, 1992.

Elyada YM, Haag J, Borst A. Different receptive fields in axons and dendrites underlie robust coding in motion-sensitive neurons. *Nat Neurosci* 12: 327–332, 2009.

Fan RJ, Marin-Burgin A, French KA, Otto FW. A dye mixture (Neurobiotin and Alexa 488) reveals extensive dye-coupling among neurons in leeches; physiology confirms the connections. *J Comp Physiol A Neuroethol Sens Neural Behav Physiol* 191: 1157–1171, 2005.

Farrow K, Borst A, Haag J. Sharing receptive fields with your neighbors: tuning the vertical system cells to wide field motion. *J Neurosci* 25: 3985–3993, 2005.

Farrow K, Haag J, Borst A. Nonlinear, binocular interactions underlying flow field selectivity of a motion-sensitive neuron. *Nat Neurosci* 9: 1312–1320, 2006.

Fischbach KF, Dittrich APM. The optic lobe of *Drosophila melanogaster*. I. A Golgi analysis of wild-type structure. *Cell Tissue Res* 258: 441–475, 1989.

Fry SN, Rohrseitz N, Straw AD, Dickinson MH. Visual control of flight speed in *Drosophila melanogaster*. *J Exp Biol* 212: 1120–1130, 2009.

Frye MA, Dickinson MH. Fly flight: a model for the neural control of complex behavior. *Neuron* 32: 385–388, 2001.

Frye MA, Dickinson MH. Closing the loop between neurobiology and flight behavior in *Drosophila*. *Curr Opin Neurobiol* 14: 729–736, 2004.

Geiger G, Nässel DR. Visual orientation behaviour of flies after selective laser beam ablation of interneurones. *Nature* 293: 398–399, 1981.

Gilbert C, Gronenberg W, Strausfeld NJ. Oculomotor control in calliphorid flies: head movements during activation and inhibition of neck motor neurons corroborate neuroanatomical predictions. *J Comp Neurol* 361: 285–297, 1995.

Gilbert C, Strausfeld NJ. The functional organization of male-specific visual neurons in flies. *J Comp Physiol A Sens Neural Behav Physiol* 169: 395–411, 1991.

Götz KG. Optomotorische Untersuchungen des visuellen Systems einiger Augenmutanten der Fruchtfliege Drosophila. *Kybernetik* 2: 77–92, 1964.

Götz KG. Die optischen Übertragungseigenschaften der Komplexaugen von Drosophila. *Kybernetik* 2: 215–221, 1965.

Götz KG, Buchner E. Evidence for one-way movement detection in the visual system of *Drosophila*. *Biol Cybern* 31: 243–248, 1978.

Gouwens NW, Wilson RI. Signal propagation in *Drosophila* central neurons. *J Neurosci* 29: 6239–6249, 2009.

Gronenberg W, Strausfeld NJ. Descending neurons supplying the neck and flight motor of diptera: physiological and anatomical characteristics. *J Comp Neurol* 302: 973–991, 1990.

Haag J, Borst A. Recurrent network interactions underlying flow-field selectivity of visual interneurons. *J Neurosci* 21: 5685–5692, 2001.

Haag J, Borst A. Dendro-dendritic interactions between motion-sensitive large-field neurons in the fly. *J Neurosci* 22: 3227–3233, 2002.

Haag J, Borst A. Neural mechanism underlying complex receptive field properties of motion-sensitive interneurons. *Nat Neurosci* 7: 628–634, 2004.

Haag J, Borst A. Dye-coupling visualizes networks of large-field motion-sensitive neurons in the fly. *J Comp Physiol A Sens Neural Behav Physiol* 191: 445–454, 2005.

Haag J, Borst A. Reciprocal inhibitory connections within a neural network for rotational optic-flow processing. *Front Neurosci* 1: 111–121, 2007.

Haag J, Borst A. Electrical coupling of lobula plate tangential cells to a heterolateral motion-sensitive neuron in the fly. *J Neurosci* 28: 14435–14442, 2008.

Haag J, Denk W, Borst A. Fly motion vision is based on Reichardt detectors regardless of the signal-to-noise ratio. *Proc Natl Acad Sci USA* 101: 16333–16338, 2004.

Haag J, Wertz A, Borst A. Integration of lobula plate output signals by DNOVS1, an identified premotor descending neuron. *J Neurosci* 27: 1992–2000, 2007.

Hausen K. Motion sensitive interneurons in the optomotor system of the fly. I. The horizontal cells: structure and signals. *Biol Cybern* 45: 143–156, 1982a.

Hausen K. Motion sensitive interneurons in the optomotor system of the fly. II. The horizontal cells: receptive field organization and response characteristics. *Biol Cybern* 46: 67–79, 1982b.

Hausen K, Wehrhahn C. Neural circuits mediating visual flight control in flies. I. Quantitative comparison of neural and behavioral response characteristics. *J Neurosci* 9: 3828–3836, 1989.

Heisenberg M. Comparative behavioral studies on 2 visual mutants of *Drosophila*. *J Comp Physiol* 80: 119–136, 1972.

Heisenberg M, Buchner E. The role of retinula cell types in visual behavior of *Drosophila melanogaster*. *J Comp Physiol* 117: 127–162, 1977.

Heisenberg M, Wolf R. *Vision in Drosophila.* New York: Springer-Verlag, 1984.

Heisenberg M, Wonneberger R, Wolf R. Optomotor-blind (H31): a *Drosophila* mutant of the lobula plate giant neurons. *J Comp Physiol* 124: 287–296, 1978.

Hengstenberg R, Hausen K, Hengstenberg B. The number and structure of giant vertical cells (VS) in the lobula plate of the blowfly Calliphora erytrocephala. *J Comp Physiol A Sens Neural Behav Physiol* 149: 163–177, 1982.

Horstmann W, Egelhaaf M, Warzecha AK. Synaptic interaction increase optic flow specificity. *Eur J Neurosci* 12: 2157–2165, 2000.

Joesch M, Plett J, Borst A, Reiff DF. Response properties of motion-sensitive visual interneurons in the lobula plate of *Drosophila melanogaster*. *Curr Biol* 18: 1–7, 2008.

Katsov AY, Clandinin TR. Motion processing streams in *Drosophila* are behaviorally specialized. *Neuron* 59: 322–335, 2008.

Kern R, van Hateren JH, Michaelis C, Lindemann JP, Egelhaaf M. Function of a fly motion-sensitive neuron matches eye movements during free flight. *PLoS Biol* 3: e171, 2005.

Krapp HG, Hengstenberg B, Hengstenberg R. Dendritic structure and receptive-field organization of optic flow processing interneurons in the fly. *J Neurophysiol* 79: 1902–1917, 1998.

Krapp HG, Hengstenberg R, Egelhaaf M. Binocular contributions to optic flow processing in the fly visual system. *J Neurophysiol* 85: 724–734, 2001.

Mronz M, Lehmann FO. The free-flight response of *Drosophila* to motion of the visual environment. *J Exp Biol* 211: 2026–2045, 2008.

Nordström K, Barnett PD, Moyer de Miguel I, Brinkworth RSA, O'Carroll DC. Sexual dimorphism in the hoverfly motion vision pathway. *Curr Biol* 18: 661–667, 2008.

O'Carroll D, Bidwell NJ, Laughlin SB, Warrant EJ. Insect motion detectors matched to visual ecology. *Nature* 382: 63–66, 1996.

Otsuna H, Ito K. Systematic analysis of the visual projection neurons of *Drosophila melanogaster*. I. Lobula-specific pathways. *J Comp Neurol* 497: 928–958, 2006.

Raghu SV, Joesch M, Borst A, Reiff DF. Synaptic organization of lobula plate tangential cells in *Drosophila*: gamma-aminobutyric acid receptors and chemical release sites. *J Comp Neurol* 502: 598–610, 2007.

Raghu SV, Joesch M, Sigrist SJ, Borst A, Reiff DF. Synaptic organization of lobula plate tangential cells in Drosophila: Dalpha7 cholinergic receptors. *J Neurogenet* 23: 200–209, 2009.

Reichardt W. Autocorrelation, a principle for the evaluation of sensory information by the central nervous system. In: *Sensory Communication*, edited by Rosenblith WA. New York: MIT Press/Wiley, 1961, p. 303–317.

Reichardt W, Egelhaaf M. Properties of individual movement detectors as derived from behavioural experiments on the visual system of the fly. *Biol Cybern* 58: 287–294, 1988.

Rister J, Pauls D, Schnell B, Ting CY, Lee CH, Sinakevitch I, Morante J, Strausfeld NJ, Ito K, Heisenberg M. Dissection of the peripheral motion channel in the visual system of *Drosophila melanogaster*. *Neuron* 56: 155–170, 2007.

Scott EK, Raabe T, Luo LQ. Structure of the vertical and horizontal system neurons of the lobula plate in *Drosophila*. *J Comp Neurol* 454: 470–481, 2002.

Single S, Borst A. Dendritic integration and its role in computing image velocity. *Science* 281: 1848–1850, 1998.

Single S, Haag J, Borst A. Dendritic computation of direction selectivity and gain control in visual interneurons. *J Neurosci* 17: 6023–6030, 1997.

Strausfeld NJ. *Atlas of an Insect Brain*. Berlin: Springer-Verlag, 1976.

Strausfeld NJ. Functional neuroanatomy of the blowfly's visual system. In: *Photoreception and Vision in Invertebrates*, edited by Ali MA. New York: Plenum, 1984, p. 483–522.

Tammero LF, Frye MA, Dickinson MH. Spatial organization of visuomotor reflexes in *Drosophila*. *J Exp Biol* 207: 113–122, 2004.

Warzecha AK, Egelhaaf M, Borst A. Neural circuit tuning fly visual interneurons to motion of small objects. I. Dissection of the circuit by pharmacological and photoinactivation techniques. *J Neurophysiol* 69: 329–339, 1993.

Wertz A, Haag J, Borst A. Local and global motion preferences in descending neurons of the fly. *J Comp Physiol A Neuroethol Sens Neural Behav Physiol* 195: 1107–1120, 2009.

Wilson RI, Laurent G. Role of GABAergic inhibition in shaping odor-evoked spatiotemporal patterns in the *Drosophila* antennal lobe. *J Neurosci* 25: 9069–9079, 2005.

Wilson RI, Turner GC, Laurent G. Transformation of olfactory representations in the *Drosophila* antennal lobe. *Science* 303: 366–370, 2004.

Zhu Y, Nern A, Zipursky SL, Frye MA. Peripheral visual circuits functionally segregate motion and phototaxis behaviors in the fly. *Curr Biol* 19: 613–619, 2009.